Effects of Energy-Band Structures on Longitudinal Magnetoacoustic Phenomena in Bismuth

Chih-Chong Wu

College of Engineering,

National Chiao Tung University,

Hsinchu, Taiwan, China

Jensan Tsai

Institute of Nuclear Science,

National Tsing Hua University,

Hsinchu, Taiwan, China

and

Chung-Chan Wu

Preparatory School,

National Overseas Chinese Student University,

Luchow, Taiwan, China

(Received 5 November 1974)

The effects of energy-band structures on the propagation of ultrasound in bismuth in the presence of a dc magnetic field are investigated by using the quantum-mechanical treatment which is valid in the high-frequency region. It is found that the absorption coefficient and change in sound velocity oscillate with the dc magnetic field for the Cohen nonellipsoidal nonparabolic (NENP) model. However, no oscillations in the absorption coefficient can be observed in strong magnetic fields for both ellipsoidal nonparabolic (ENP) and ellipsoidal parabolic (EP) models. These oscillations can be interpreted as the so-called "giant quantum oscillations" which arise from the resonant absorption of the sound wave by electrons. It is also found that the absorption coefficient and change in sound velocity increase with the sound frequency for NENP, ENP, and EP models. However, there exists a big discontinuous cusp at the high-frequency region for both ENP and EP models. Therefore we conclude that the NENP model will give a much better description of the energy band structure in bismuth than do the ENP and EP models.

1. INTRODUCTION

Although some early works have demonstrated that the Fermi surface for electrons in bismuth can be satisfactorily described by the ellipsoidal parabolic (EP) model, [1] some later works [2-12] have indicated that the Fermi surface in bismuth may be a two-band model. Moreover, several works [4-10] have shown that the magnetic field dependence of some physical phenomena in bismuth can be explained using a two-band model for the energy band structure. From theoretical calculations [11] and experimental results, [6,7,10] it was pointed out that the energy band in bismuth structure is the Cohen nonellipsoidal nonparabolic (NENP) model. However, the magnetooptical results of Maltz and Dresselhaus [12] supported the Lax ellipsoidal nonparabolic (ENP) model.[2] It is the purpose of this paper to investigate the effects of energy-band structures on longitudinal magnetoacoustic phenomena in bismuth. We compare some numerical results of the absorption coefficient and change in sound velocity for the NENP model with those for the ENP and EP models, and find out which kind of models is the best description of the energy band structure in bismuth. We focus attention on the role of the deformation potential in determining the acoustic attenuation. The intersting temperature in our present case is assumed to be near absolute zero. We study this problem using a quantum-mechanical treatment which is valid at high frequencies and in strong magnetic fields. Since we are interested in the high-frequency region such that $\omega\tau \gg 1$, where ω is the sound frequency and τ is the relaxation time of electrons. Consequently, the effect of collisions is neglected.

In Section 2, we follow the previous paper [13] to find the longitudinal ac conductivity tensor for the NENP model in the presence of a dc magnetic field $\vec{B}$. We also present the results for the ENP and EP models. In Section 3 we present some numerical results for the absorption coefficient and sound velocity in bismuth. We also give a brief discussion of our numerical results by considering the energy band structures as the NENP, ENP, and EP models.

2. LONGITUDINAL CONDUCTIVITY TENSORS

For convenience, we shall first consider the case without including the electron spin-splitting effect. In the NENP model, the energy eigenvalue equation for electrons in a uniform dc magnetic field $\vec{B}$ directed along the z direction is

$$H_0(1+H_0/E_g)\,\psi_{kns} = (1/2m)[\alpha_1 p_x^2 + \alpha_2(p_y - eBx/c)^2 + \alpha_3 p_z^2$$

$$+\alpha_4(p_y-eBx/c)^4]\phi_{\vec{k}_n}$$

$$=E_{\vec{k}}(1+E_{\vec{k}}/E_g)\phi_{\vec{k}_n} \quad , \qquad (1)$$

where m is the mass of the free electron, E_g is the energy gap between the L-point valence and conduction bands, $E_{\vec{k}_n}$ is the true energy of the system defined by $H_0\phi_{\vec{k}_n}=E_{\vec{k}_n}\phi_{\vec{k}_n}$, and some parameters α_1, α_2, α_3, and α_4 are defined as follows:

$$\alpha_1=m/m_1 \quad ,$$

$$\alpha_2=(m/m_2)\,[1+(E_{\vec{k}_n}/E_g)(1-m_2/m_2')]\cong m/m_2 \quad ,$$

$$\alpha_3=m/m_3 \quad , \qquad (2)$$

and

$$\alpha_4=\frac{m}{2m_2m_2'E_g} \quad ,$$

where m_1, m_2, and m_3 are the effective-mass tensor components at the bottom of the L-point conduction band, and m_2' is an effective-mass tensor component at the top of the L-point valence band. From experimental results,[7, 10, 14] it has been indicated that the difference between m_2 and m_2' is quite small, i.e., $m_2\approx m_2'$. Then, by considering $H'=(\alpha_4/2m)\ (p_y-eBx/c)^4$ as a perturbation term, the eigenfunctions and eigenvalues up to first order for Eq. (1) are given by

$$\phi_{\vec{k}_n}(\vec{r})=\exp(ik_yy+ik_zz)\{\phi_n(x-x_0)+(\delta/16\hbar\omega_c)[n(n-1)(n-2)(n-3)]^{1/2}$$
$$\times\phi_{n-4}(x-x_0)+(\delta/4\hbar\omega_c)[n(n-1)]^{1/2}(2n-1)\phi_{n-2}(x-x_0)$$
$$-(\delta/4\hbar\omega_c)[(n+1)(n+2)]^{1/2}(2n+3)\phi_{n+2}(x-x_0)$$
$$-(\delta/16\hbar\omega_c)[(n+1)(n+2)(n+3)(n+4)]^{1/2}\phi_{n+4}(x-x_0)\}, \qquad (3)$$

and

$$E_{\vec{k}_n}=-\tfrac{1}{2}E_g\Big(1-\{1+(4/E_g)[(n+\tfrac{1}{2})\hbar\omega_c+\hbar^2k_z^2/2m^*+\frac{3}{2}\delta\ (n^2+n+\tfrac{1}{2})]\}^{1/2}\Big) \quad , \qquad (4)$$

where $\omega_c=(|e|B/mc)(\alpha_1\alpha_2)^{1/2}$, $\delta=(\alpha_1\alpha_4/\alpha_2)(e^2B^2\hbar^2/2mc^2)$, $x_0=\hbar ck_y/eB$, $m^*=m/\alpha_3$, and $\phi_n(x)$ is the harmonic-oscillator wave function.

If the electron spin-splitting effect is taken into account, the eigenfunctions become

$$\phi_{\vec{k}_n s}(\vec{r})=\begin{pmatrix}\frac{1+s}{2}\\ \frac{1-s}{2}\end{pmatrix}\phi_{\vec{k}_n}(\vec{r}) \quad , \qquad (5)$$

where $\phi_{\vec{k}_n}(\vec{r})$ are given by Eq. (3) and $s=\pm 1$. Similarly, the eigenvalues of the system are given by

$$\sigma_{zz}(\overrightarrow{q},\omega)=\frac{i(\omega_p^*)^2\omega(m^*)^{3/2}}{8\sqrt{2}\pi\hbar q^3\sum_{n,s}(\triangle E_{ns}')^{1/2}}\sum_{n,s}a_{ns}'$$

$$\times\Big\{ln\Big(\frac{(\triangle E_{ns}')^{1/2}+q\hbar/2\sqrt{2}(m^*)^{1/2}-\omega(m^*)^{1/2}a_{ns}'/\sqrt{2}q}{-(\triangle E_{ns}')^{1/2}+q\hbar/2\sqrt{2}(m^*)^{1/2}-\omega(m^*)^{1/2}a_{ns}'/\sqrt{2}q}\Big)$$

$$-ln\Big(\frac{(\triangle E_{ns}')^{1/2}-q\hbar/2\sqrt{2}(m^*)^{1/2}-\omega(m^*)^{1/2}a_{ns}'/\sqrt{2}q}{-(\triangle E_{ns}')^{1/2}-q\hbar/2\sqrt{2}(m^*)^{1/2}-\omega(m^*)^{1/2}a_{ns}'/\sqrt{2}q}\Big)\Big\}\ , \qquad (10)$$

where $\triangle E_{ns}'=E_F(1+E_F/E_g)-(n+\frac{1}{2})\hbar\omega_c-(s/2)\hbar\omega_s$ and $a_{ns}'=\{1+(4/E_g)[(n+\frac{1}{2})\hbar\omega_c+(s/2)\hbar\omega_s]\}^{1/2}$.

In the EP model, the conductivity tensor σ_{zz} can be obtained from Eq. (10) by putting $a_{ns}'=1$ and changing $\triangle E_{ns}'$ to $\triangle E_{ns}''=E_F-(n+\frac{1}{2})\hbar\omega_c-(s/2)\hbar\omega_s$.

It is assumed that the interaction between the ultrasound and conduction electrons in bismuth is via deformation potential coupling. Then the relation between the absorption coefficient and the ac conductivity tensor $\sigma_{zz}(\overrightarrow{q},\omega)$ for one type of carrier being dominant in the presence of the dc magnetic field is given by[17]

$$\alpha_{11}=-\frac{\varepsilon}{4\pi\rho v_s^2}\Big(\frac{\omega}{v_s}\Big)^3\Big(\frac{C}{e}\Big)^2 Im\Big(1-\frac{4\pi\sigma_{zz}(\overrightarrow{q},\omega)}{i\omega\varepsilon}\Big)^{-1}\ , \qquad (11)$$

where ρ is the density of the material, ε is the static dielectric constant, v_s is the sound velocity, and C is the deformation potential. The change in the sound velocity due to the interaction between the ultrasound and conduction electrons is also related to the ac counductivity tensor $\sigma_{zz}(\overrightarrow{q},\omega)$,

$$\frac{\triangle v_s}{v_s}=\frac{\varepsilon}{8\pi\rho v_s^2}\Big(\frac{\omega}{v_s}\Big)^2\Big(\frac{C}{e}\Big)^2 Re\Big(1-\frac{4\pi\sigma_{zz}(\overrightarrow{q},\omega)}{i\omega\varepsilon}\Big)^{-1}\ , \qquad (12)$$

3. NUMERICAL RESULTS AND DISCUSSION

In this section we present some numerical results for the absorption coefficient of ultrasound and the change in sound velocity in bismuth at very-low-temperature limits. The numerical values of physical parameters for bismuth are [18, 19] $n_0=2.75\times10^{17}$ cm^{-3} , $\alpha_1=172$, $\alpha_2=0.8$, $\alpha_3=88.5$, $E_g=0.0153\,eV$, $E_F=0.0276\ eV$, $C=10\ eV$, $\varepsilon=10$, $\rho=9.86\ g/cm^3$, and $v_s=10^5$ cm/sec.

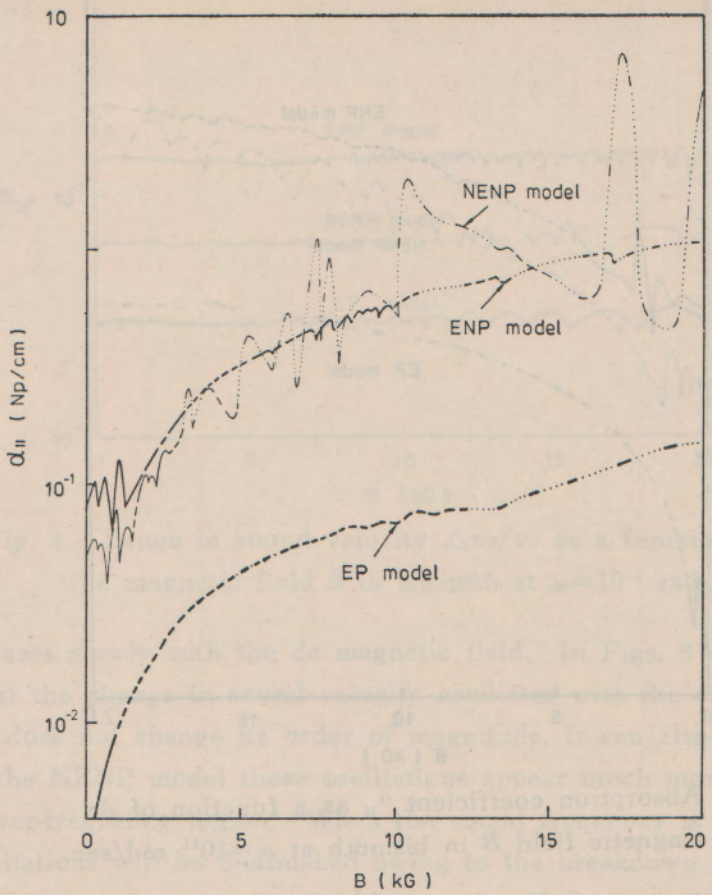

Fig. 1. Absorption coefficient α_{11} as a function of dc magnetic field B in bismuth at $\omega=5\times10^{10}$ rad/sec.

In Figs. 1 and 2, it is shown that the absorption coefficient oscillates with the dc magnetic field and some discontinuities can be observed for the NENP model as the energy band in bismuth. However, these oscillations will be diminished with increasing the sound frequency. We can also see that no oscillations in the absorption coefficient can be observed in strong magnetic fields for both ENP and EP models as the energy bands in bismuth. It can be seen that the absorption coefficient for NENP, ENP, and EP mo-

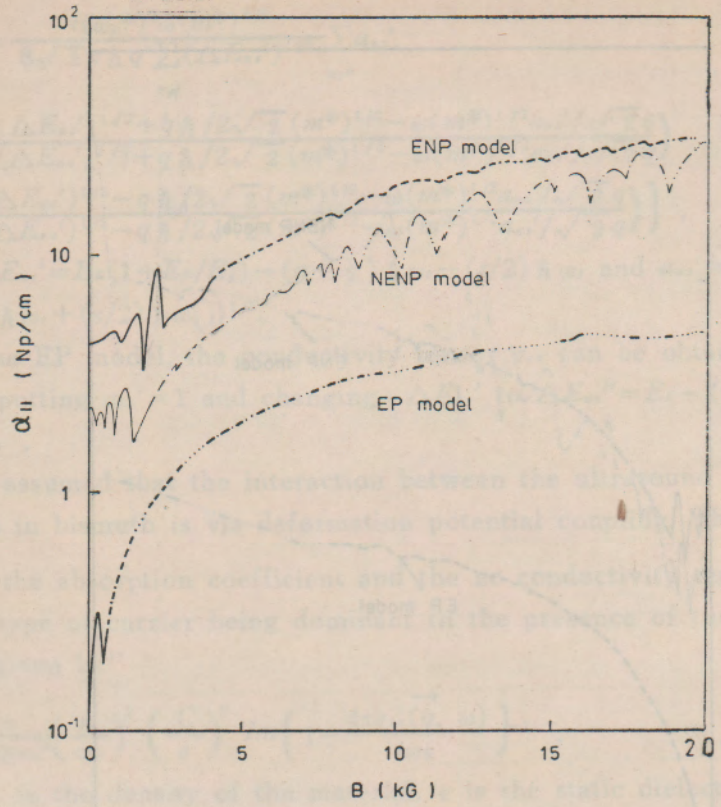

Fig. 2. Absorption coefficient α_{11} as a function of dc magnetic field B in bismuth at $\omega=10^{11}$ rad/sec.

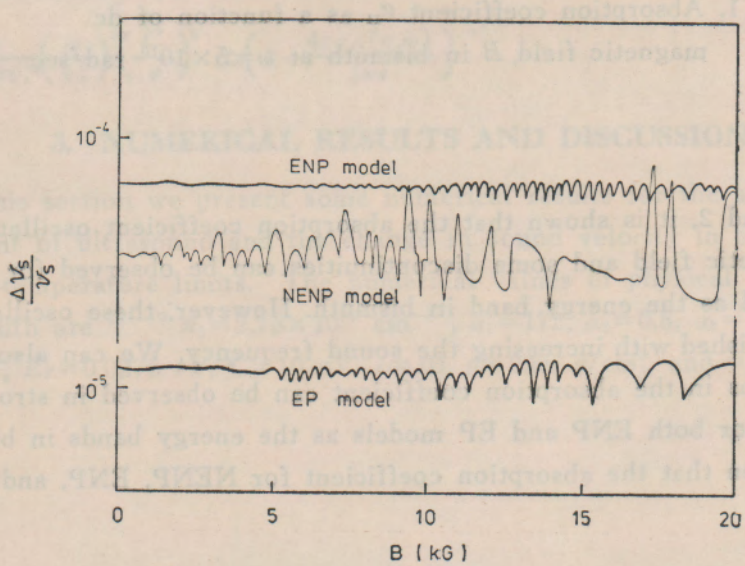

Fig. 3. Change in sound velocity $\Delta v_s/v_s$ as a function of dc magnetic field B in bismuth at $\omega=5\times10^{10}$ rad/sec.

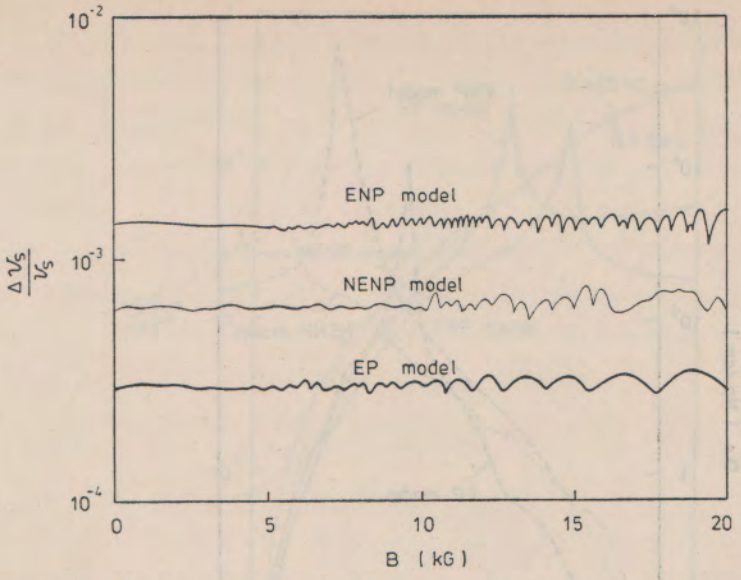

Fig. 4. Change in sound velocity $\Delta v_s/v_s$ as a function of dc magnetic field B in bismuth at $\omega=10^{11}$ rad/sec.

dels increases slowly with the dc magnetic field. In Figs. 3 and 4, it is shown that the change in sound velocity oscillates with the dc magnetic field, but does not change its order of magnitude. It can also be seen that only for the NENP model these oscillations appear much more considerably at the lower-frequency region. When the sound frequency is increasing, these oscillations will be diminished owing to the breakdown of the screening. However, we can not see any enhancement of these oscillations for both ENP and EP models. In Figs. 5 and 6, we plot the absorption coefficient α_{11} as a function of the sound frequency in bismuth at $B=5$ kG, 10 kG, respectively. It is shown that the absorption coefficient will be increasing with the sound frequency and then decreasing. There exists a big cusp at the high-frequency region for both ENP and EP models. For the NENP model the cusp disappears, but there exists a maximum point in the neighborhood of $\omega=2.4\times10^{11}$ rad/sec. In Fig. 7, we show the change in sound velocity will also be increasing with the sound frequency. Again the big cusp will appear in the case of the ENP or EP model. Moreover, only curves for the NENP model can be split out with the the dc magnetic field. For the ENP or EP model, the change in the sound velocity can not be split out considerably with the dc magnetic field.

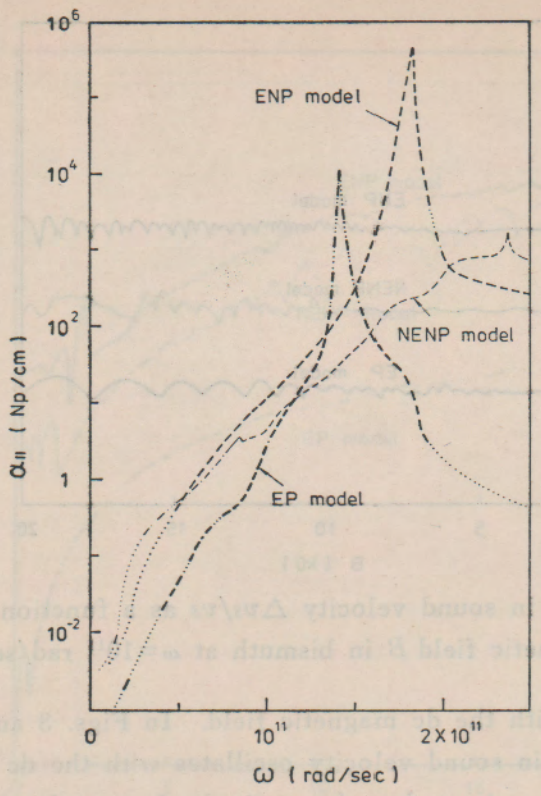

Fig. 5. Absorption coefficient α_{11} as a function of sound frequency ω in bismuth at $B=5k$G.

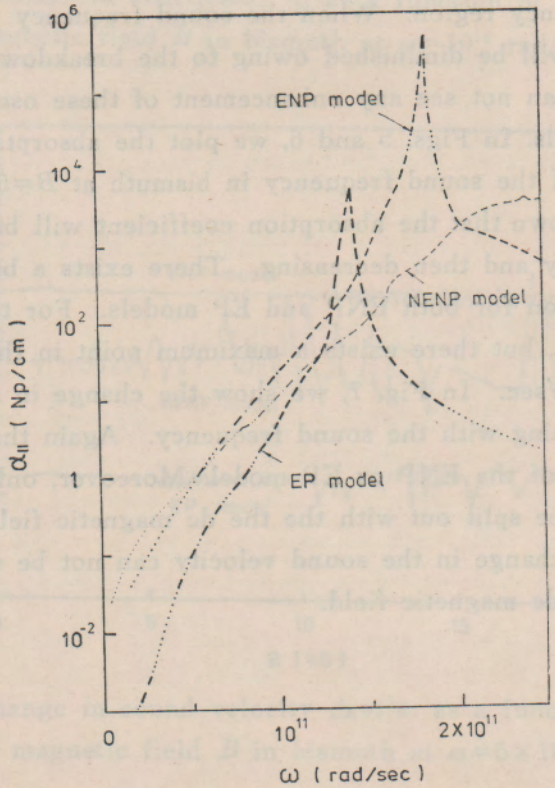

Fig. 6. Absorption coefficient α_{11} as a function of sound frequency ω in bismuth at $B=10k$G.

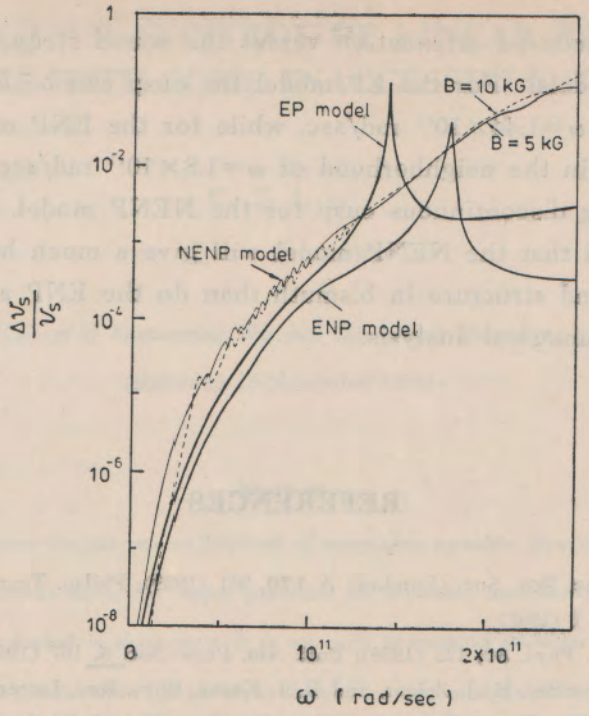

Fig. 7. Change in sound velocity $\Delta v_s/v_s$ as a function of sound frequency ω in bismuth.

From the results of our numerical analysis presented here, it is shown that the absorption coefficient and change in the sound velocity of the longitudinal ultrasound travelling parallel to the dc magnetic field exhibit oscillations as a function of the dc magnetic field. As the sound frequency increases, these oscillations are diminished considerably due to the breakdown of the screening. Since we are interested in the frequencies in the microwave region such that $\omega\tau \gg 1$, therefore these oscillations can be interpreted as the so-called "giant quantum oscillations".[17, 20-22] These giant quantum oscillations arise from the resonant absorption of the sound wave by electrons which move along the dc magnetic field with the sound velocity. Therefore these oscillations occur in a degenerate electron gas in the case when the electron level is near the Fermi surface and the sound wave vector $\vec{q}$ has a component along the dc magnetic field. However, no oscillations of the acoustic absorption with the dc magnetic field can be observed for both ENP and EP models as the energy bands of bismuth in strong magnetic fields. It can also be found that some discontinuities in the absorption coefficient are shown to vanish owing to the real part of the longitudinal conductivity tensor being zero. This means that no energy can be transferred between the conduction electrons and sound wave in bismuth in some regions of the dc magnetic field and sound frequency. There exists an abnormal

big cusp in the acoustic attenuation versus the sound frequency for both ENP and EP models. For the EP model the cusp can be observed in the neighborhood of $\omega = 1.44 \times 10^{11}$ rad/sec, while for the ENP model the cusp can be observed in the neighborhood of $\omega = 1.8 \times 10^{11}$ rad/sec. However, we can not see a big discontinuous cusp for the NENP model. Therefore, it can be concluded that the NENP model will give a much better description of the energy band structure in bismuth than do the ENP and EP models in our present numerical analysis.

REFERENCES

1. D. Shoenberg, Proc. Roy. Soc. (London) A **170,** 341 (1939); Philso. Trans. Roy. Soc. (London) A **245,** 1 (1952).
2. B. Lax, Rev. Mod. Phys. **30,** 122 (1958); Bull. Am. Phys. Soc. **5,** 167 (1960).
3. B. Lax, J. G. Mavroides, H. J. Zeiger, and R. J. Keyes, Phys. Rev. Letters **5,** 241 (1960).
4. Yu. M. Gal'perin, Fiz. Tverd. Tela **10,** 2338 (1968) [Sov. Phys.-Solid State **10,** 1840 (1969)].
5. M. Giura, R. Marcon, T. Papa, and F. Wanderlingh, Nuovo Cimento B **63,** 192 (1969).
6. J. F. Koch and J. D. Jensen, Phys. Rev. **184,** 643 (1969).
7. R. J. Dinger and A. W. Lawson, Phys. Rev. A **1,** 2418 (1670); Phys. Rev. B **3,** 253 (1971).
8. V. Ya. Demikhovskii and A. P. Kopasov, Fiz. Tverd.Tela **13,** 2468 (1971) [Sov. Phys.-Solid State **13,** 2068 (1972)].
9. U. Strom, A. Kamgar, and J. F. Koch, Phys. Rev. B **7,** 2435 (1973).
10. R. J. Dinger and A. W. Lawson, Phys. Rev. B **7,** 5215 (1973).
11. M. H. Cohen, Phys. Rev. **121,** 387 (1961).
12. M. Maltz and M. S. Dresselhaus, Phys. Rev. B **2,** 2877 (1970).
13. Chhi-Chong Wu and J. Tsai, Phys. Rev. B **5,** 4008 (1972).
14. G. A. Antcliffe and R. T. Bate, Phys. Rev. **160,** 531 (1967).
15. M. H. Cohen and E. I. Blount, Philos. Mag. **5,** 115 (1960).
16. G. A. Baraff, Phys. Rev. **137,** A 842 (1965).
17. H. N. Spector, in "Solid State Physics", edited by F. Seitz and D. Turnbull (Academic, New York, 1966), Vol. 19, p. 291.
18. M. J. Harrison, Phys. Rev. **119,** 1260 (1960).
19. L. A. Fal' kovskii, Usp. Fiz. Nauk **94,** 3 (1968) [Sov. Phys.- Usp. **11,** 1 (1969)].
20. V. L. Gurevich, V. G. Skobov, and Yu. A. Firsov, Zh. Eksp. Teor. Fiz. **40,** 786 (1961) [Sov. Phys.-JETP **13,** 552 (1961)].
21. S. H. Liu and A. M. Toxen, Phys. Rev. **138,** A 487. (1965).
22. F. G. Bass and I. B. Levinson, Zh. Eksp. Teor. Fiz. **49,** 914 (1965) [Sov. Phys.-JETP **22,** 635 (1966)].